Dalton Transactions

ROYAL SOCIETY OF CHEMISTRY

PAPER

View Article Online
View Journal | View Issue

Cite this: *Dalton Trans.*, 2022, **51**, 8009

Shape dependent photocatalytic H_2 evolution of a zinc porphyrin†

Emmanouil Orfanos, [a] Kalliopi Ladomenou, *[b] Panagiotis Angaridis [c] and Athanassios G. Coutsolelos *[a,d]

Received 21st February 2022,
Accepted 29th April 2022

DOI: 10.1039/d2dt00556e

rsc.li/dalton

Hydrogen is regarded as a promising molecular fuel in order to produce clean energy, thus it is of great importance to produce and store H_2 in order to replace fossil fuels and to resolve the global energy and environmental problems. One strategy to produce hydrogen is the photocatalytic splitting of water. In this study different supramolecular architectures of a Zn(II) porphyrin, showing "flower", octahedral and "manta ray" shaped structures, were obtained using the "good-bad" solvent self-assembly protocol. More specifically, the bad solvent (methanol) was retained and the good solvent was alerted obtaining diverse assemblies. The different structures were studied by scanning electron microscopy, PXRD, UV-Vis and IR spectroscopies. The prepared structures were capable of proton reduction and production of molecular H_2 in the presence of 5% w/w Pt-nanoparticles as catalysts and ascorbic acid as a sacrificial electron donor. Moreover, depending on the structure of the chromophore that is formed the amount of H_2 produced varies. The maximum H_2 production was obtained with the octahedral structures (185.5 μmol g^{-1} h^{-1}).

Introduction

Porphyrins are extensively present in nature and play important roles in life. These molecules are well known to self-associate or aggregate in order to form different size and shape organized structures, following simple methodologies. These altered structures influence their optical properties compared to their monomers. Therefore, inspired by nature where porphyrins are organized in a specific manner, synthetic porphyrinic analogues have been broadly studied in order to understand their mechanisms of aggregation and to explore varied applications. Some of these applications include, artificial photosynthesis, photovoltaics, catalysis, non-covalent synthesis, artificial enzymes *etc.*[1–5] Moreover, porphyrins feature chemical stability, facile structural modification, photochemical and photophysical properties, making them attractive structures for photocatalytic applications, especially for photocatalytic hydrogen evolution.[6] Hence, the use of self-assembled porphyrin derivatives features well defined structures in specific arrangements able to enhance the light absorption, to improve the charge carriage and to be able to block charge recombination in order to improve the H_2 production. Hydrogen is an ideal solar fuel, upon its combustion is formed just water, and comprise high energy density.[7] One way to produce hydrogen is through the photocatalytic water splitting, where a photosensitizer, a catalyst and an electron donor are the essential constituents of this procedure. In solar hydrogen production a plethora of porphyrins have been mainly used as photosensitizers. However, most metalated porphyrins are generally used in homogenous catalysis where the use of organic solvents is essential in order to dissolve them, limiting the transfer of photoinduced electrons in the aqueous phase for hydrogen production. Inspired by the light harvesting properties in nature, one way to overcome this problem is the formation and use of self-assembled structures of chromophores. This kind of structures can be prepared following different self-assembly protocols. For example, evaporation, organogelation, interfacial assembly, reprecipitation, molecular recognition, surfactant assisted self-assembly *etc.*[8,9] Metalated porphyrins are a class of ideal molecules to self-assemble due to their planar molecular skeleton and their aromatic features. In general, self-assembled chromophores demonstrate different properties compared to their monomers, making them an attractive approach in the field of photocatalytic hydrogen evolution.[10,11] Our group, has prepared and studied many self-

[a]*University of Crete, Department of Chemistry, Laboratory of Bioinorganic Chemistry, Voutes Campus, 70013 Heraklion, Crete, Greece. E-mail: acoutsol@uoc.gr*
[b]*International Hellenic University, Department of Chemistry, Laboratory of Inorganic Chemistry, Agios Loucas, 65404, Kavala Campus, Greece*
[c]*Aristotle University of Thessaloniki, Department of General and Inorganic Chemistry, Faculty of Chemistry, GR-54124 Thessaloniki, Greece*
[d]*Institute of Electronic Structure and Laser (IESL) Foundation for Research and Technology - Hellas (FORTH), Vassilika Vouton, GR 70013 Heraklion, Crete, Greece*

†Electronic supplementary information (ESI) available. CCDC 2153314. For ESI and crystallographic data in CIF or other electronic format see DOI: **https://doi.org/10.1039/d2dt00556e**

assembled porphyrin derivatives and our latest reports are in the field of hydrogen evolution.[12–20] There are a few examples reported in the literature in the field of the photocatalytic hydrogen production, where the self-assembled structures feature greater photocatalytic activity compared to the monomeric species, possibly due to their enhanced light capture.[21–25]

In this report we synthesized a simple zinc(II) tetraphenyl porphyrin, **ZnTPP** and studied three different self-assembled architectures obtained with the use of a "bad"/"good" solvent protocol. Then we investigated the impact of the different shapes formed, in hydrogen evolution experiments under visible light irradiation.

Results and discussion

The self-assembly architectures were visualized with scanning electron microscopy (SEM) and the structures were obtained following the "good-bad" solvent protocol.[26] In this approach we just varied the "good" solvent and we kept constant both: (a) the "bad" solvent and (b) the ratio between the two solvents. Initially, **ZnTPP** was dissolved in the "good" solvent such as chloroform ($CHCl_3$), tetrahydrofuran (THF), and toluene (Tol) and then the "bad" solvent methanol (MeOH) was added in 1 : 4 "good"/"bad" solvent ratio and in 2.9 mM concentration, at room temperature. We selected the "good" solvents with varied polarity starting with the most polar tetrahydrofuran following the order THF > $CHCl_3$ > Tol. We wanted to investigate how the different polarity of the solvent affects the structures that formed and subsequently examine how the hydrogen production would be affected, upon the photocatalytic reactions of each component. As illustrated in Fig. 1, in each solvent mixture **ZnTPP** porphyrin was able to form different shaped structures. When the most polar solvent THF was used as the good solvent (THF/MeOH 1 : 4), well-shaped octahedral type of architectures was obtained (Fig. 1(a)). The growth of porphyrin molecules formed assemblies with *ca.* 20–40 μm width and *ca.* 50–80 μm length. Then, with the same porphyrin **ZnTPP** "flower" like structures were formed by just changing the "good" solvent with *ca.* 5–15 μm diameter (Fig. 1(b)). Once the less polar solvent Tol was used "manta-ray" type structures were observed (Fig. 1(c)). The diameter of this structure was *ca.* 15–20 μm and 40–50 μm length. Therefore, the same porphyrin can form three distinctive structures by just alerting the "good" solvent. The presence of the polar, protic solvent MeOH assist in the formation of architectures. In the literature similar type of structures of **ZnTPP** have already been reported in $CHCl_3$/MeOH, 1 : 1 mixture.[9] The formation of diverse structures using the same zinc porphyrin depends on the solvent's polarity and volatility. Therefore the intermolecular interactions (π–π and van der Waals) of the porphyrin moieties differ according to the solvent changing the intermolecular interactions and the kinetics of the assembly formation. The difference in the solvent's polarity and volatility leads the same porphyrin to self-assemble in different ways and form diverse aggreagate structures.

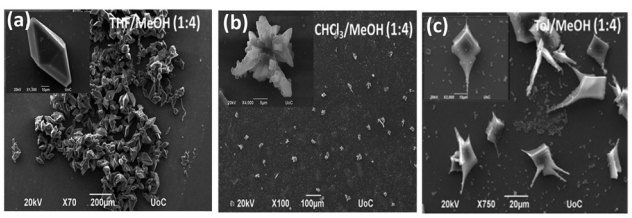

Fig. 1 Supramolecular architectures with different morphologies of **ZnTPP**: (a) octahedral (THF/MeOH 1 : 4), (b) "flower" ($CHCl_3$/MeOH 1 : 4), (c) "manta-ray" (Tol/MeOH 1 : 4).

The formation of the structures was monitored by UV-Vis and fluorescence spectroscopies as a function of time. A certain amount of solution was obtained from the reaction vial at different time intervals 0 h, 0.5 h, 4 h, 24 h, and 48 h. Then, the UV-Vis (Fig. S1–S3†) and the fluorescence spectra (Fig. S5–S7†) were recorded. Moreover, the spectra in the good solvents were obtained (Fig. S4†), showing the characteristic porphyrin absorbances. The Soret band of the porphyrin is alerting as a function of time suggesting that the porphyrin aggregates. In all cases, after 48 h the absorption intensity of the Soret was diminished and only in the case of $CHCl_3$/MeOH the band was red shifted by 4 nm. This finding indicates the formation of *J*-type aggregates (edge-to-edge).[4,27] In addition, the emission spectra of **ZnTPP** in all samples showed two characteristic emission peaks at 604 nm and 655 nm and a significant quenching after 48 h, that reached to 50% in the case of the octahedral structures, once again due to the formation of aggregates. Moreover, the fluorescence spectra in the solid state of the three structures were obtained (Fig. S8†). In the case of "manta-ray" type structures two emission peaks were detected, where the second emission peak is significantly reduced compared to the corresponding peak in the solution. The octahedral and the "flower" like structures appear to have three emission peaks.

Time-resolved fluorescence lifetime measurements were recorded (Table S1†). It is well known in the literature that the most common values of singlet excited-state lifetime (τ) for **ZnTPP** are in the range 1.8–2.2 ns.[28] The lifetime measurements of **ZnTPP** that were performed in CH_2Cl_2 and in the $CHCl_3$/MeOH, 1 : 4 mixture during the formation of the different structures were in the same range as reported in the literature (Table S1†). The fluorescence decays for all porphyrinic structures in solid state were calculated by using a double-exponential function with satisfactory data fitting. The fractional amplitudes of shorter lifetimes (0.58, 0.70, 0.76 ns) are decreased from 70% for octahedral to 66% for "flower" and to 60% for "manta ray". The value of **ZnTPP** in CH_2Cl_2 was τ = 1.97 ns, that is in the range of the longer lifetimes of the solid structures (1.96, 2.46, 2.49 ns), for octahedral, "flower" and "manta-ray", respectively. Therefore, this higher value is attributed to the Zn porphyrin, whereas the shorter lifetimes can be ascribed to the ordered structure formation in the solid state. The lifetimes of the "flower" and "manta-ray" structures in

solid state were longer compared to the solution. Therefore, the self-organization changed the features of the **ZnTPP** porphyrin in both ground and excited state. Even though, the similarity in short and long lifetimes of "flower" and "manta-ray", the "manta-ray" structure produced more H_2 during the photocatalysis probably due to its enhanced stability as shown in the SEM experiments (Fig. S11†).

FT-IR spectroscopy was performed of all three different structures in order to compare their structural features. (Fig. S9†) As appeared in the spectra the features of "flowers", octahedral and "manta-ray" are similar confirming that they all have the same composition. All the above experimental results are in accordance to the literature, where a mechanism for similar ordered aggregation of metalloporphyrins was proposed.[9] Dominant role on the type of the molecular packing conformation plays the π–π interactions and the metal–ligand coordination.

The different self-assembled structures of **ZnTPP** formed from the above-mentioned solvent mixtures were examined by powder X-ray diffraction (PXRD) analysis. The experimentally obtained PXRD patterns of the three samples are depicted in Fig. 2. Indexing and space group determination were not possible to be performed. A comparative analysis with simulated powder diffraction patterns of crystal structures analogous to **ZnTPP** that have been determined by single crystal X-ray diffraction analysis and deposited in the Cambridge Crystallographic Data Centre (CCDC) database was ineffective, since none of them gave good match with the experimentally obtained diffraction patterns of the diffraction patterns of the three synthesized forms of **ZnTPP**.

However, it can be clearly seen that "flower" and "manta-ray" forms of **ZnTPP** display very similar PXRD patterns, demonstrating good agreement in the general positions of specific diffraction peaks (*e.g.* at 2θ = 8.1°, 10.3°, 20.6°, and 27.1°). In contrast, octahedral form of **ZnTPP** show a totally different diffraction pattern. This difference proves the determining effect of the solvents used in each case on the formation of particular architectures. Taking into account the strong Lewis base character of MeOH and THF used in our solvent mixtures, their coordination to the Zn(II) centers of **ZnTPP** is expected to affect porphyrin's self-assembly and potentially lead to different architectures (due to differences in the steric properties of the two solvents). Along these lines, the similarity of the PXRD patterns of "flower" and "manta-ray" **ZnTPP** structures can be attributed to the coordination of MeOH (that is present in the corresponding solvent mixtures) to the Zn(II) centers of **ZnTPP** molecules, which can lead to mono- and/or bis-MeOH adducts. On the contrary, octahedral **ZnTPP**, obtained from the THF/MeOH solvent system, should be considered as a result of the coordination of THF to the Zn(II) centers. Interestingly, the PXRD pattern of octahedral **ZnTPP** structure is not the same with the simulated diffraction pattern obtained from the crystal structure of **ZnTPP**$(THF)_2$ that we determined experimentally by single-crystal X-ray diffraction analysis (for details of crystal structure determination and molecular structure parameters see ESI†).[29] An analogous crystal structure of this bis-THF adduct was reported in the past which, however, displayed slightly different crystallographic parameters and geometrical characteristics.[30] Therefore, in the case of the octahedral **ZnTPP** structure, except from THF, MeOH is also expected to play an important role in the self-assembly process possibly by affecting the development of intermolecular interactions of **ZnTPP** molecules and the kinetics of the self-assembly.

The catalytic performance of the three **ZnTPP** architectures towards H_2 production under photocatalytic conditions in water was investigated. All three components were obtained by complete removal of the organic solvents in the air. This material was used as a photosensitizer and Pt nanoparticles as catalyst. The Pt nanoparticles were formed by photo-deposition of 5% w/w $Na_2PtCl_6{\cdot}6H_2O$ on the porphyrin material (the exact procedure is described in ESI†).

The photocatalytic experiments of the three different samples in solid state, were studied in aqueous solution in the presence of 1 M ascorbic acid as a sacrificial electron donor, at pH = 4. In Fig. 3 are presented all H_2 evolution experiments of the different solids. The highest performance was obtained for the octahedral 185.5 μmol g^{-1} h^{-1}. The "flower" structure gave the lowest hydrogen production 44.4 μmol g^{-1} h^{-1} and the "manta-ray" shapes 166 μmol g^{-1} h^{-1}. These results indicate that the different structural formation affect the H_2 evolution, therefore with just a simple chromophore we can significantly improve its efficiency by just varying the solvents during the self-assembly procedure. When just Pt nanoparticles were used under the same conditions in the absence of porphyrin, no H_2 formation was detected.

After the photochemical reactions (8 h of irradiation) additional SEM studies were performed in order to examine if the porphyrin structures were altered. The SEM images are shown in Fig. 4, where in all cases the structures were completely transformed, featuring amorphous structures. In order to understand the cause of this structural alteration after the photocatalytic experiments, further research was performed. Firstly, three different mixtures of good/bad solvent were prepared and irradiated for 8 h in the absence of catalyst (Pt) and SED (ascorbic acid). The SEM images showed that the light

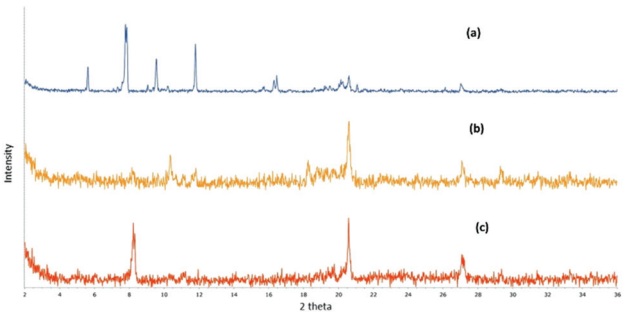

Fig. 2 PXRD patterns of different supramolecular architectures of **ZnTPP**: (a) octahedral (THF/MeOH 1 : 4), (b) "flower" ($CHCl_3$/MeOH 1 : 4), (c) "manta-ray" (Tol/MeOH 1 : 4).

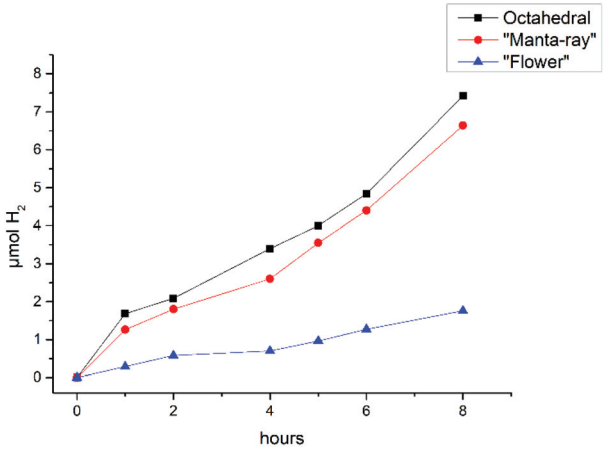

Fig. 3 Photocatalytic hydrogen production plots of 5 mg **ZnTPP** with different shape in the presence of Pt nanoparticles (using $Na_2PtCl_6{\cdot}6H_2O$ as a platinum source). The photocatalytic experiments were performed in aqueous ascorbic acid 1 M at pH = 4. The results presented in the plots are the average values of three independent measurements within (4–10% error).

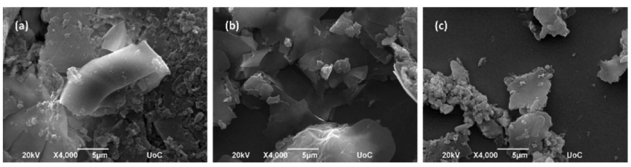

Fig. 4 Supramolecular architectures with different morphologies of **ZnTPP** formed after photocatalytic experiments: (a) octahedral (THF/MeOH 1 : 4), (b) "flower" ($CHCl_3$/MeOH 1 : 4), (c) "manta-ray" (Tol/MeOH 1 : 4).

irradiation alerted the obtained structures since there images were completely different compared to the initial structures, as shown in Fig. S10.† Therefore, the light irradiation is able to destroy the structures of **ZnTPP**. Secondly, in the three initial structures water, ascorbic acid 1 M and 5% w/w $Na_2PtCl_6{\cdot}6H_2O$ were added and left stirring in the dark for 8 h. Then, the SEM images were obtained, after the removal of the SED by washing the structures with water (three times), following by centrifugation in order to separate the solid. This procedure might alert the form of the initial structures as well. Subsequently, the SEM images were obtained as shown in Fig. S11.† The octahedral structure in THF/MeOH remained almost the same, the "manta-ray" in Tol/MeOH appeared different whereas the "flower" like structure in $CHCl_3$/MeOH was completely different. Therefore, the octahedral and the "manta-ray" type of structures seem to be more stable in the photocatalytic conditions, in the absence of light irradiation. Possibly this is the reason that both structures produce more H_2 compared to the "flower" type structure. Nevertheless, the porphyrins can be recycled and reused, following the same synthetic protocol, for additional photocatalytic experiments producing almost the same amount of H_2.

Conclusions

The photocatalytic hydrogen evolution from water using three different self-assembled structures of the same Zn(II)-porphyrin as photosensitizers is reported in this work. Their preparation, characterization and self-assembled behaviour was studied. In particular, by using the same "bad" solvent and just alerting the "good" solvent, different structures were obtained: "flower", octahedral and "manta ray" shaped structures. The three structures featured different catalytic activities towards H_2 production. The octahedral type of structure demonstrated the maximum H_2 evolution rate of 185.5 μmol g^{-1} h^{-1} that is more than 4 times greater compared to "flower" structure. The porphyrin can be recycled, modified again in the most efficient assembly for H_2 production. With this research work, simple porphyrin-based chromophores can be altered by appropriate self-organization using mix solvents in order to enhance their photocatalytic H_2 evolution.

Author contributions

Emmanouil Orfanos, synthesis and characterization, Kalliopi Ladomenou, characterization and writing the ms, Panagiotis Angaridis, X-ray analysis, Athanassios G. Coutsolelos, idea, writing ms.

Conflicts of interest

"There are no conflicts to declare".

Acknowledgements

This research was funded by the General Secretariat for Research and Technology (GSRT) and Hellenic Foundation for Research and Innovation (HFRI; project code: 508). This research has also been co-financed by the European Union and Greek national funds through the Operational Program Competitiveness, Entrepreneurship, and Innovation, under the call RESEARCH– CREATE–INNOVATE (project code: T1EDK-01504). In addition, this research has been co-financed by the European Union and Greek national funds through the Regional Operational Program "Crete 2014-2020", project code OPS:5029187. Moreover, the European Commission's Seventh Framework Program (FP7/2007-2013) under grant agreement no. 229927 (FP7-REGPOT-2008-1, Project BIO-SOLENUTI) and the Special Research Account of the University of Crete are gratefully acknowledged for the financial support of this research.

References

1 M. C. O'Sullivan, J. K. Sprafke, D. V. Kondratuk, C. Rinfray, T. D. W. Claridge, A. Saywell, M. O. Blunt, J. N. O'Shea,

P. H. Beton, M. Malfois and H. L. Anderson, Vernier templating and synthesis of a 12-porphyrin nano-ring, *Nature*, 2011, **469**(7328), 72–75.

2 I. Beletskaya, V. S. Tyurin, A. Y. Tsivadze, R. Guilard and C. Stern, Supramolecular Chemistry of Metalloporphyrins, *Chem. Rev.*, 2009, **109**(5), 1659–1713.

3 P. Thordarson, E. J. A. Bijsterveld, A. E. Rowan and R. J. M. Nolte, Epoxidation of polybutadiene by a topologically linked catalyst, *Nature*, 2003, **424**(6951), 915–918.

4 K. Ogawa, T. Zhang, K. Yoshihara and Y. Kobuke, Large Third-Order Optical Nonlinearity of Self-Assembled Porphyrin Oligomers, *J. Am. Chem. Soc.*, 2002, **124**(1), 22–23.

5 G. Steinberg-Yfrach, P. A. Liddell, S.-C. Hung, A. L. Moore, D. Gust and T. A. Moore, Conversion of light energy to proton potential in liposomes by artificial photosynthetic reaction centres, *Nature*, 1997, **385**(6613), 239–241.

6 K. Ladomenou, M. Natali, E. Iengo, G. Charalampidis, F. Scandola and A. G. Coutsolelos, Photochemical hydrogen generation with porphyrin-based systems, *Coord. Chem. Rev.*, 2015, **304–305**, 38–54.

7 X. Chen, S. Shen, L. Guo and S. S. Mao, Semiconductor-based Photocatalytic Hydrogen Generation, *Chem. Rev.*, 2010, **110**(11), 6503–6570.

8 S. S. Babu, S. Prasanthkumar and A. Ajayaghosh, Self-Assembled Gelators for Organic Electronics, *Angew. Chem., Int. Ed.*, 2012, **51**(8), 1766–1776.

9 J. Cai, H. Chen, J. Huang, J. Wang, D. Tian, H. Dong and L. Jiang, Controlled self-assembly and photovoltaic characteristics of porphyrin derivatives on a silicon surface at solid–liquid interfaces, *Soft Matter*, 2014, **10**(15), 2612–2618.

10 K. C. Peters, S. Mekala, R. A. Gross and K. D. Singer, Chiral inversion and enhanced cooperative self-assembly of bio-surfactant-functionalized porphyrin chromophores, *J. Mater. Chem. C*, 2020, **8**(14), 4675–4679.

11 Y. Liu, H. Wang, S. Li, C. Chen, L. Xu, P. Huang, F. Liu, Y. Su, M. Qi, C. Yu and Y. Zhou, In situ supramolecular polymerization-enhanced self-assembly of polymer vesicles for highly efficient photothermal therapy, *Nat. Commun.*, 2020, **11**(1), 1724.

12 E. Nikoloudakis, K. Mitropoulou, G. Landrou, G. Charalambidis, V. Nikolaou, A. Mitraki and A. G. Coutsolelos, Self-assembly of aliphatic dipeptides coupled with porphyrin and BODIPY chromophores, *Chem. Commun.*, 2019, **55**(94), 14103–14106.

13 E. Nikoloudakis, K. Karikis, J. Han, C. Kokotidou, A. Charisiadis, F. Folias, A. M. Douvas, A. Mitraki, G. Charalambidis, X. Yan and A. G. Coutsolelos, A self-assembly study of PNA–porphyrin and PNA–BODIPY hybrids in mixed solvent systems, *Nanoscale*, 2019, **11**(8), 3557–3566.

14 E. Nikoloudakis, K. Karikis, M. Laurans, C. Kokotidou, A. Solé-Daura, J. J. Carbó, A. Charisiadis, G. Charalambidis, G. Izzet, A. Mitraki, A. M. Douvas, J. M. Poblet, A. Proust and A. G. Coutsolelos, Self-assembly study of nanometric spheres from polyoxometalate-phenylalanine hybrids, an experimental and theoretical approach, *Dalton Trans.*, 2018, **47**(18), 6304–6313.

15 G. Charalambidis, K. Karikis, E. Georgilis, B. L. M'Sabah, Y. Pellegrin, A. Planchat, B. Lucas, A. Mitraki, J. Bouclé, F. Odobel and A. G. Coutsolelos, Supramolecular architectures featuring the antenna effect in solid state DSSCs, *Sustainable Energy Fuels*, 2017, **1**(2), 387–395.

16 K. Karikis, E. Georgilis, G. Charalambidis, A. Petrou, O. Vakuliuk, T. Chatziioannou, I. Raptaki, S. Tsovola, I. Papakyriacou, A. Mitraki, D. T. Gryko and A. G. Coutsolelos, Corrole and Porphyrin Amino Acid Conjugates: Synthesis and Physicochemical Properties, *Chem. – Eur. J.*, 2016, **22**(32), 11245–11252.

17 G. Charalambidis, E. Georgilis, M. K. Panda, C. E. Anson, A. K. Powell, S. Doyle, D. Moss, T. Jochum, P. N. Horton, S. J. Coles, M. Linares, D. Beljonne, J.-V. Naubron, J. Conradt, H. Kalt, A. Mitraki, A. G. Coutsolelos and T. S. Balaban, A switchable self-assembling and disassembling chiral system based on a porphyrin-substituted phenylalanine–phenylalanine motif, *Nat. Commun.*, 2016, **7**(1), 12657.

18 G. Charalambidis, E. Kasotakis, T. Lazarides, A. Mitraki and A. G. Coutsolelos, Self-Assembly Into Spheres of a Hybrid Diphenylalanine–Porphyrin: Increased Fluorescence Lifetime and Conserved Electronic Properties, *Chem. – Eur. J.*, 2011, **17**(26), 7213–7219.

19 V. Nikolaou, G. Charalambidis, K. Ladomenou, E. Nikoloudakis, C. Drivas, I. Vamvasakis, S. Panagiotakis, G. Landrou, E. Agapaki, C. Stangel, C. Henkel, J. Joseph, G. Armatas, M. Vasilopoulou, S. Kennou, D. M. Guldi and A. G. Coutsolelos, Controlling Solar Hydrogen Production by Organizing Porphyrins, *ChemSusChem*, 2021, **14**(3), 961–970.

20 V. Nikolaou, G. Charalambidis and A. G. Coutsolelos, Photocatalytic hydrogen production of porphyrin nanostructures: spheres vs. fibrils, a case study, *Chem. Commun.*, 2021, **57**(33), 4055–4058.

21 G. B. Bodedla, J. Huang, W.-Y. Wong and X. Zhu, Self-Assembled Naphthalimide-Substituted Porphyrin Nanowires for Photocatalytic Hydrogen Evolution, *ACS Appl. Nano Mater.*, 2020, **3**(7), 7040–7046.

22 N. Zhang, L. Wang, H. Wang, R. Cao, J. Wang, F. Bai and H. Fan, Self-Assembled One-Dimensional Porphyrin Nanostructures with Enhanced Photocatalytic Hydrogen Generation, *Nano Lett.*, 2018, **18**(1), 560–566.

23 G. B. Bodedla, L. Li, Y. Che, Y. Jiang, J. Huang, J. Zhao and X. Zhu, Enhancing photocatalytic hydrogen evolution by intramolecular energy transfer in naphthalimide conjugated porphyrins, *Chem. Commun.*, 2018, **54**(82), 11614–11617.

24 J. Wang, Y. Zhong, L. Wang, N. Zhang, R. Cao, K. Bian, L. Alarid, R. E. Haddad, F. Bai and H. Fan, Morphology-Controlled Synthesis and Metalation of Porphyrin Nanoparticles with Enhanced Photocatalytic Performance, *Nano Lett.*, 2016, **16**(10), 6523–6528.

25 Y. Zhong, S. Liu, J. Wang, W. Zhang, T. Tian, J. Sun and F. Bai, Self-assembled supramolecular nanostructure

photosensitizers for photocatalytic hydrogen evolution, *APL Mater.*, 2020, **8**(12), 120706.

26 K. Karikis, A. Butkiewicz, F. Folias, G. Charalambidis, C. Kokotidou, A. Charisiadis, V. Nikolaou, E. Nikoloudakis, J. Frelek, A. Mitraki and A. G. Coutsolelos, Self-assembly of (boron-dipyrromethane)-diphenylalanine conjugates forming chiral supramolecular materials, *Nanoscale*, 2018, **10**(4), 1735–1741.

27 G. Lu, X. Zhang, X. Cai and J. Jiang, Tuning the morphology of self-assembled nanostructures of amphiphilic tetra(p-hydroxyphenyl)porphyrins with hydrogen bonding and metal–ligand coordination bonding, *J. Mater. Chem.*, 2009, **19**(16), 2417–2424.

28 M. Taniguchi, J. S. Lindsey, D. F. Bocian and D. Holten, Comprehensive review of photophysical parameters (ε, Φf, τs) of tetraphenylporphyrin (H2TPP) and zinc tetraphenylporphyrin (ZnTPP) – Critical benchmark molecules in photochemistry and photosynthesis, *J. Photochem. Photobiol., C*, 2021, **46**, 100401.

29 A. G. Coutsolelos, E. Orfanos, K. Ladomenou and P. Angaridis, in *CCDC 2153314: Experimental Crystal Structure Determination*, 2022.

30 C. K. Schauer, O. P. Anderson, S. S. Eaton and G. R. Eaton, Crystal and molecular structure of a six-coordinate zinc porphyrin: bis(tetrahydrofuran)(5,10,15,20-tetraphenylporphinato)zinc(II), *Inorg. Chem.*, 1985, **24**(24), 4082–4086.